ISSN 1063-7826, Semiconductors, 2018, Vol. 52, No. 11, pp. 1424–1427. © Pleiades Publishing, Ltd., 2018.
Original Russian Text © O.A. Novodvorsky, V.A. Mikhalevsky, D.S. Gusev, A.A. Lotin, L.S. Parshina, O.D. Khramova, E.A. Cherebylo, A.B. Drovosekov, V.V. Rylkov, S.N. Nikolaev, K.Yu. Chernoglazov, K.I. Maslakov, 2018, published in Fizika i Tekhnika Poluprovodnikov, 2018, Vol. 52, No. 11, pp. 1313–1316.

XXII INTERNATIONAL SYMPOSIUM "NANOPHYSICS AND NANOELECTRONICS", NIZHNY NOVGOROD, MARCH 12–15, 2018

Modification of the Ferromagnetic Properties of $Si_{1-x}Mn_x$ Thin Films Synthesized by Pulsed Laser Deposition with a Variation in the Buffer-Gas Pressure

O. A. Novodvorsky[a,*], V. A. Mikhalevsky[a], D. S. Gusev[a], A. A. Lotin[a], L. S. Parshina[a], O. D. Khramova[a], E. A. Cherebylo[a], A. B. Drovosekov[b], V. V. Rylkov[c,d], S. N. Nikolaev[c], K. Yu. Chernoglazov[c], and K. I. Maslakov[e]

[a] *Institute of Laser and Information Technologies—Branch of the Federal Scientific Research Center "Crystallography and Photonics", Russian Academy of Sciences, Shatura, 140700 Russia*

[b] *Kapitza Institute for Physical Problems, Russian Academy of Sciences, Moscow, 119334 Russia*

[c] *National Research Center "Kurchatov Institute", Moscow, 123182 Russia*

[d] *Fryazino Branch of the Kotelnikov Institute of Radioengineering and Electronics, Russian Academy of Sciences, Fryazino, 141190 Russia*

[e] *Moscow State University, Moscow, 119991 Russia*

**e-mail: onov@mail.ru*

Submitted April 25, 2018; accepted for publication May 7, 2018

Abstract—A series of thin films of $Si_{1-x}Mn_x$ alloys with a thickness from 50 to 100 nm grown by pulsed laser deposition on an Al_2O_3 substrate in vacuum and in an argon atmosphere is investigated. The significant effect of the buffer-gas pressure in the sputtering chamber on the structural and magnetic homogeneity of the obtained films is shown. The conditions for the formation of a ferromagnetic phase with a high Curie temperature (>300 K) in the samples are studied. With the use of the Langmuir probe method, the threshold of ablation of a MnSi target by second harmonic radiation ($\lambda = 532$ nm) of a Nd:YAG Q-switch laser is determined. The time-of-flight curves for the plume ions are obtained with a change in the energy density at the target and argon pressure in the sputtering chamber. A nonmonotonic dependence of the probe time-of-flight signal amplitude on the argon pressure is established for high-energy particles of the plume.

DOI: 10.1134/S1063782618110179

1. INTRODUCTION

Silicon-containing thin-film magnetic semiconductors are attractive for the development of elements of spintronics, since they can be readily integrated in modern microelectronic technology [1]. Recently, the possibility of increasing the density of elements in data storage and processing devices based on helical ferromagnets was revealed [2]. One such material is ε-MnSi, in which, at a temperature of 26 to 28 K, somewhat lower than the Curie point $T_C = 29.5$ K, stable arrays of isolated magnetization vortices, so-called magnetic skyrmions, were discovered. These magnetic skyrmions are capable of moving at low current densities (~10^2 A/cm^2) [3, 4]. A short while ago, it was established that, in thin-film samples of $Si_{1-x}Mn_x$ with a small excess of Mn ($x = 0.52$–0.55) obtained by pulsed laser deposition (PLD), the Curie temperature is $T_C \geq 300$ K; i.e., a small deviation from the stoichiometric composition of MnSi leads to an order of magnitude increase in the T_C value compared to that of ε-MnSi [5, 6]. Later investigations [7, 8] revealed that these films, in addition to a high-temperature ferromagnetic (FM) phase, can include a low-temperature FM phase, the formation of which can depend on both the energy of deposited particles and the value of nonstoichiometry of the $Si_{1-x}Mn_x$ films. Therefore, controlling the particle energy during deposition and the possibility of a controlled variation in the $Si_{1-x}Mn_x$ film composition are an important issue in obtaining single-phase thin-film samples with a high Curie temperature. In the present work, to tackle this issue, a series of $Si_{1-x}Mn_x$ thin films obtained by a droplet-free PLD technique at different argon pressures in a sputtering chamber are investigated.

2. RESULTS AND THEIR DISCUSSION

Using argon as a buffer gas, which possesses an atomic weight close to that of silicon and manganese, makes it possible to decrease the energy of particles leaving the target in the process of ablation and change

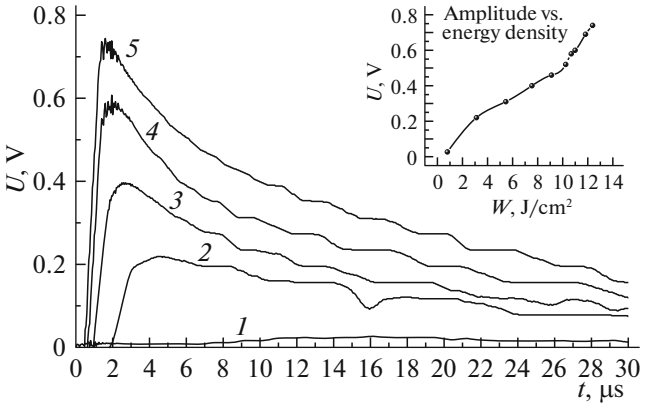

Fig. 1. Time-of-flight probe curves obtained for various energy densities W for a MnSi target subjected to ablation: (*1*) 0.8, (*2*) 3.1, (*3*) 7.5, (*4*) 10.7, and (*5*) 12.4 J/cm^2. In the inset, the probe-signal amplitude versus the energy density W at the target is shown.

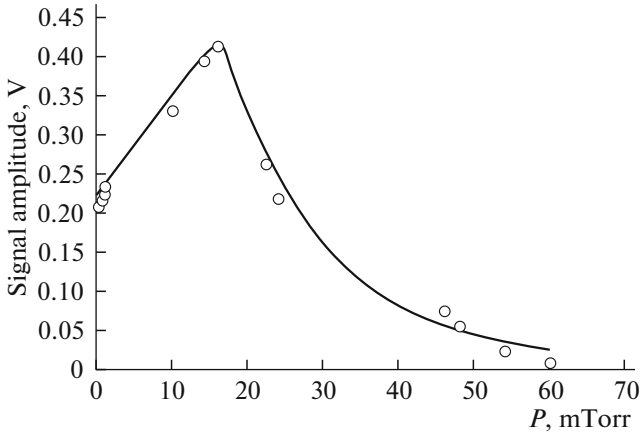

Fig. 2. Time-of-flight probe-signal amplitude of the MnSi target versus the argon pressure. The dots are the experimental data and the line is the approximation.

the diagram of their expansion, which provides a smooth variation in the deposited-film composition. By means of the Langmuir probe technique, the velocity distribution function of charged particles of the plume at different argon pressures was determined. Figure 1 shows the time-of-flight probe curves (time dependences of the probe-signal amplitude) obtained when a MnSi target was ablated with the second harmonic radiation (λ = 532 nm) of a Q-switched Nd:YAG laser; the curves demonstrate the impact of the energy density at the target in the range of W = 0.7–12.4 J/cm^2. The probe signal increases steadily within the entire considered time range. The probe investigations allowed us to determine the threshold energy density of target ablation, which is W = 0.8 J/cm^2.

The amplitude of the probe time-of-flight signal for high-energy particles of the plume depends on two factors [9]: (I) the ionization of argon atoms upon collisions with high-energy manganese and silicon ions and (II) the scattering of plume ions at atoms of the buffer gas (argon). The first mechanism, increasing the probe-signal amplitude, dominates at low argon pressures, and the second mechanism, decreasing the probe signal, starts to dominate with an increase in the buffer-gas pressure. For this reason, the dependence of the probe time-of-flight signal amplitude on the argon pressure for high-energy particles of the plume is nonmonotonic (Fig. 2). The nonmonotonic dependence of the probe time-of-flight signal amplitude on the argon pressure for high-energy particles of the plume is determined by the combined contribution of these two processes. The effect of an increase in the signal amplitude is observed at such pressures when the free path of plume ions with an energy higher than the ionization potential of an argon atom is longer or comparable to the probe–target distance. A decrease in the signal amplitude is observed at higher argon pressures.

The time-of-flight signal of the probe current is expressed as [10]

$$i(t) = 0.5sen(t)v,$$

where s is the probe's lateral surface area, e is the elementary charge, and v is the velocity of ions near the probe. The velocity of ions arriving at the probe at the moment t is

$$v(t) = l/t,$$

and the time-of-flight signal can be expressed through the charge-density distribution in the plume passing by the probe

$$n(t) = 2i(t)t/(sel),$$

where l is the probe–target distance. From the time-of-flight curves, the distribution functions of charged particles over the emission velocity are determined for different buffer-gas (argon) pressures in the vacuum chamber, which is illustrated in Fig. 3. With increasing buffer-gas pressure, the concentration of charged particles on the plume axis decreases due to scattering at atoms of the buffer gas and the velocity of charged particles decreases because of collisions.

To reveal the optimal conditions for obtaining single-phase $Si_{1-x}Mn_x$ ferromagnetic layers with a Curie temperature apt for practical applications, their composition, structural features, and electrophysical and magnetic properties are investigated.

The composition and structure of the films were investigated by X-ray photoelectron spectroscopy (XPS). Figure 4 illustrates the normalized spectra of the investigated $Si_{1-x}Mn_x$ samples obtained at different argon pressures (the spectra are normalized to the intensity of the Mn 3*p* line). As one can see from Fig. 4, the amplitude of the Si 2*p* peak depends on the argon pressure, which is evidence of a decrease in the

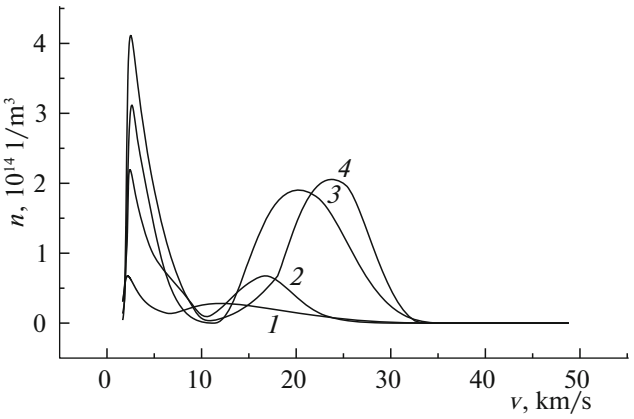

Fig. 3. Distribution function of charged particles over the expansion velocity at different buffer-gas (argon) pressures in the vacuum chamber: (*1*) 6×10^{-2}, (*2*) 4.8×10^{-2}, (*3*) 2.4×10^{-2}, and (*4*) 5.4×10^{-4} Torr. The laser energy density on the target is $W = 3$ J/cm^2.

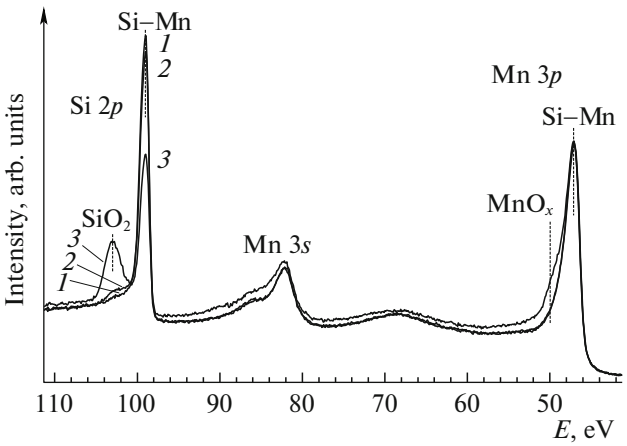

Fig. 4. Normalized XPS spectra of the investigated $Si_{1-x}Mn_x$ samples, obtained at different argon pressures P: (*1*) 8.5×10^{-6}, (*2*) 5.4×10^{-5}, and (*3*) 1.0×10^{-2} Torr.

silicon content of the $Si_{1-x}Mn_x$ films with increasing Ar pressure.

The magnetic properties of the films were studied by SQUID magnetometry and ferromagnetic resonance (FMR) in the temperature range of 4–300 K. The FMR measurements were taken at a frequency of 17.4 GHz in a magnetic field with a strength of up to 10 kOe.

The results of FMR investigations at room temperature for the series of samples $Si_{1-x}Mn_x$ obtained at different argon pressures in the sputtering chamber are shown in Fig. 5. The positions and shapes of the FMR line differ significantly for the films grown at different buffer-gas (argon) pressures. The most intense absorption peak, shifted to the left of the calculated position of paramagnetic resonance, is observed with the sample obtained at an argon pressure of $P = 8.5 \times 10^{-6}$ Torr ($W = 6.8$ J/cm^2). The other samples exhibit a weak paramagnetic peak. The most intense paramagnetic signal is that of the sample obtained at $P = 5.4 \times 10^{-4}$ Torr and $W = 7.4$ J/cm^2 (the fourth curve from the top in Fig. 5).

The temperature dependence of the demagnetization field $4\pi M_{\text{eff}}(T)$ for the sample obtained at $P = 8.5 \times 10^{-6}$ Torr ($W = 6.8$ J/cm^2) is described well by a simplified Brillouin function with a Curie point higher than room temperature $T_C \approx 310$ K (Fig. 6). Such a behavior indicates that a homogeneous high-temperature FM phase forms in the film. Additional confirmation of the homogeneity of the films grown at low P values is the behavior of the FMR line with temperature. When the temperature is decreased, the FMR shows a rather narrow absorption peak (see the inset in Fig. 6). With an increase in the buffer-gas pressure, the FMR line broadens considerably. The dependence $4\pi M_{\text{eff}}(T)$ takes on a more complicated shape

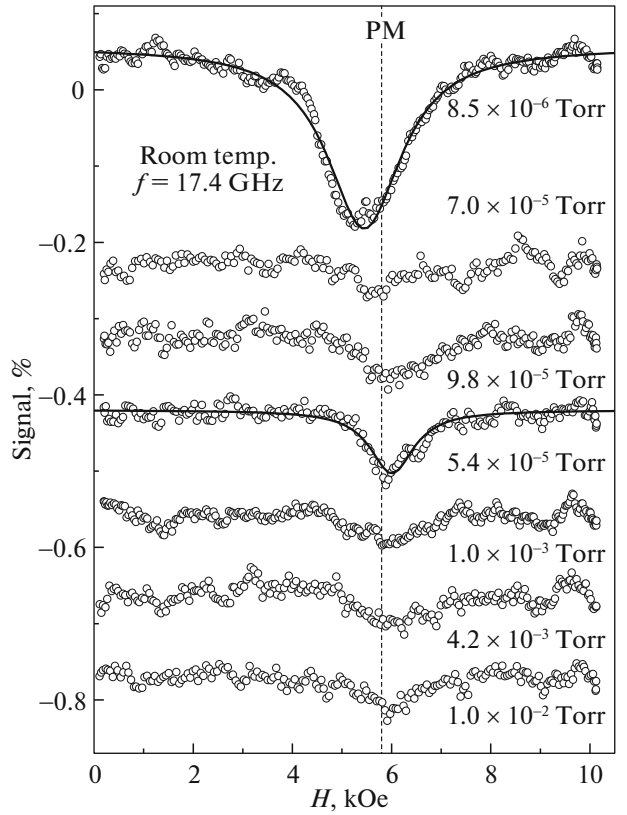

Fig. 5. Experimental ferromagnetic resonance (FMR) spectra at room temperature for $Si_{1-x}Mn_x$ films, obtained at different argon pressures in the growth chamber. The vertical dashed line marks the calculated position of the paramagnetic resonance (PM).

described by two Curie temperatures — $T_{C1} \approx 60$ K and $T_{C2} \approx 250$ K — which suggests that several FM phases coexist in the film. A further increase in the pressure P

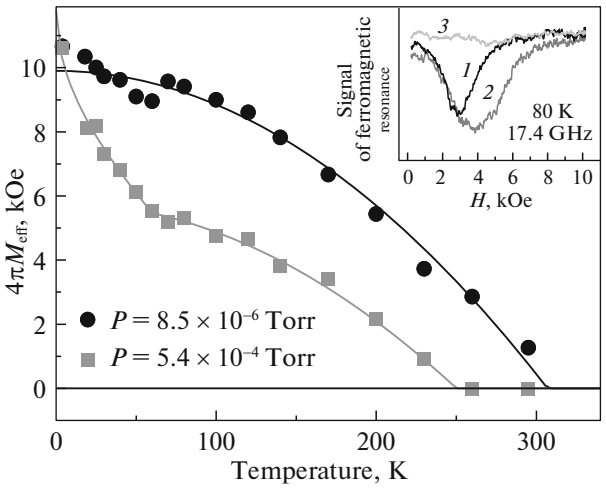

Fig. 6. Temperature dependence of the effective anisotropy field $4\pi M_{eff}$ for films grown at different buffer-gas (argon) pressures: $P = 8.5 \times 10^{-6}$ and 5.4×10^{-4} Torr. In the inset, FMR spectra for the three samples obtained at different Ar pressures are exemplified: (*1*) 8.5×10^{-6}, (*2*) 5.4×10^{-4}, and (*3*) 1.0×10^{-2} Torr.

leads to the complete suppression of ferromagnetism in the film.

3. CONCLUSIONS

In the work, the effect of the buffer-gas (argon) pressure on the composition and magnetic properties of $Si_{1-x}Mn_x$ thin films obtained by pulsed laser deposition from MnSi targets using the second harmonic radiation of a Nd:YAG laser is investigated. By means of X-ray photoelectron spectroscopy it is demonstrated that an increase in the argon pressure leads to a decrease in the relative silicon concentration in the film and a decrease in the energy of deposited particles. An unexpected result was that low buffer-gas pressures in the growth chamber and relatively high laser energy densities on the target ($W \approx 7$ J/cm^2) encourage the formation of a homogeneous high-temperature FM phase in the film. Meanwhile, an increase in the argon pressure, leading to a significant decrease in the energy of deposited particles, results in the formation of an extra low-temperature FM phase and, at the same time, favors a noticeable decrease in the Curie point for a high-temperature FM phase.

The mechanism of the influence of the energy of deposited atoms on the growth of $Si_{1-x}Mn_x$ ($x \approx 0.5$) layers is currently not completely clear. It may be possible that the results are due to a difference in the coefficients of the adhesion of Mn and Si atoms to an Al_2O_3 substrate during their deposition and a strong difference in the MnSi and Al_2O_3 substrate lattice constants (about 10% [8]), which determine the growth of smaller crystallites at high rates of MnSi deposition and the formation of a high-temperature FM phase uniform in thickness. In this context, further research is necessary, in particular, investigation of the effect of substrates (lattice mismatch) on the FM properties of $Si_{1-x}Mn_x$ ($x \approx 0.5$) layers.

ACKNOWLEDGMENTS

The work was carried out under support of the Federal Agency for Scientific Organizations (agreement no. 007-GZ/Ch3363/26) for the part "probe investigations of the plume when a MnSi target is ablated, and the synthesis of $Si_{1-x}Mn_x$ thin films" and grants of the Russian Foundation for Basic Research nos. 17-07-00615, 18-07-00772, 18-07-00756, 15-29-01171, 16-07-00657, and 16-07-00798 for the part "investigations of the electrophysical and magnetic properties of obtained nanoscale films".

REFERENCES

1. S. Zhouand and H. Schmidt, Materials **3**, 5054 (2010).
2. C. Hanneken, F. Otte, A. Kubetzka, B. Dupé, N. Romming, K. von Bergmann, R. Wiesendanger, and S. Heinze, Nat. Nanotechnol. **10**, 1039 (2015).
3. S. Mühlbauer, B. Binz, F. Jonietz, C. Pfleiderer, A. Rosch, A. Neubauer, R. Georgii, and P. Böni, Science (Washington, DC, U. S.) **323**, 915 (2009).
4. F. Jonietz, S. Mühlbauer, C. Pfleiderer, A. Neubauer, W. Münzer, A. Bauer, T. Adams, R. Georgii, P. Böni, R. A. Duine, K. Everschor, M. Garst, and A. Rosch, Science (Washington, DC, U. S.) **330**, 1648 (2010).
5. S. N. Nikolaev, V. V. Rylkov, B. A. Aronzon, K. I. Maslakov, I. A. Likhachev, E. M. Pashaev, K. Yu. Chernoglazov, N. S. Perov, V. A. Kul'bachinskii, O. A. Novodvorskii, A. V. Shorokhova, E. V. Khaidukov, O. D. Khramova, and V. Ya. Panchenko, Semiconductors **46**, 1510 (2012).
6. V. V. Ryl'kov, S. N. Nikolaev, K. Yu. Chernoglazov, B. A. Aronzon, K. I. Maslakov, V. V. Tugushev, E. T. Kulatov, I. A. Likhachev, E. M. Pashaev, A. S. Semisalova, N. S. Perov, A. B. Granovskii, O. A. Novodvorskii, O. D. Khramova, E. V. Khaidukov, and V. Ya. Panchenko, JETP Lett. **96**, 255 (2012).
7. B. A. Aronzon, A. L. Vasiliev, N. S. Perov, O. A. Novodvorsky, L. S. Parshina, M. Yu. Presniakov, and E. Lahderanta, J. Phys.: Condens. Matter **29**, 055802 (2017).
8. S. N. Nikolaev, A. S. Semisalova, V. V. Rylkov, V. V. Tugushev, A. V. Zenkevich, A. L. Vasiliev, E. M. Pashaev, K. Yu. Chernoglazov, Yu. M. Chesnokov, I. A. Likhachev, N. S. Perov, Yu. A. Matveyev, O. A. Novodvorskii, E. T. Kulatov, A. S. Bugaev, Y. Wang, and S. Zhou, AIP Adv. **6**, 015020 (2016).
9. O. A. Novodvorskii, V. A. Mikhalevskii, D. S. Gusev, A. A. Lotin, L. S. Parshina, O. D. Khramova, and E. A. Cherebylo, Tech. Phys. Lett. **44**, 271 (2018).
10. R. Kelly and W. Dreyfus, Surf. Sci. **198**, 263 (1988).

Translated by Z. Smirnova